JCTC Journal of Chemical Theory and Computation

Solvatochromic Shifts of the n → π* Transition of Acetone from Steam Vapor to Ambient Aqueous Solution: A Combined Configuration Interaction QM/MM Simulation Study Incorporating Solvent Polarization

Yen-lin Lin and Jiali Gao*

Department of Chemistry and Supercomputing Institute, Digital Technology Center, University of Minnesota, 207 Pleasant Street, SE, Minneapolis, Minnesota 55455

Received March 10, 2007

Abstract: A hybrid quantum mechanical and molecular mechanical potential is used in Monte Carlo simulations to examine the solvent effects on the electronic excitation energy of the n → π^* transition of acetone in ambient and supercritical water fluid, in which the temperature is in the range of 25−500 °C with pressures of 1−2763 atm. In the present study, the acetone molecule is described by the AM1 Hamiltonian, and the water molecules are treated classically. Two sets of calculations are performed. The first involves the TIP4P model for water, and the second employs a polarizable model, POL2, for the solvent. The first calculation yields the excitation energy by using the static ground-state solvent charge distribution obtained from QM-CI/MM calculations. The latter takes into account the effect of solvent polarization following the solute electronic excitation. The trend of the computed n → π^* blue-shifts for acetone as function of the fluid density is in good agreement with experimental results. The present simulations of acetone in the supercritical, near supercritical, dense-liquid, and ambient water fluids reveal that the solvatochromic shifts are dominated by the electrostatic interactions between acetone and water molecules during the solute excitation. Additionally, the solvent charge redistribution following the solute electronic excitation has a small correlation (0 to −37 cm^{-1}) to the total solvatochromic shift and decreases linearly with water density. Both the solvatochromic shift and solvent polarization correction are more obvious in the ambient water than in the supercritical water because the solvent stabilization of the ground state over the excited state is more significant in the former condition.

Introduction

The unusual properties of supercritical water (SCW) fluid have attracted considerable interests[1−6] as a viable medium for green chemical oxidations.[7−9] At or near supercritical conditions, organic species and molecular oxygen are completely miscible,[2−7,10,11] whereas electrolytes are nearly insoluble.[7,12] Thus, it offers a tremendous opportunity to develop alternative technologies for the destruction of chemical warfare agents and organic wastes by complete oxidation.[7,9] An advantage of performing chemical oxidations in supercritical fluid water (T_c = 374 °C, P_c = 217.7 atm, and ρ_c = 3.22 g·cm^{-3}) or near supercritical conditions is that the reaction conditions can be optimized by varying the density of the medium with a change in pressure. The variations of the fluid density, ranging from steam vapor to dense aqueous solution, also provide an interesting medium for investigating solute−solvent interactions.[13−15] The present study is aimed at an understanding of the change of solute and solvent interactions over the entire spectra of solvent density and the unusual behaviors of solvation near supercritical conditions. We focus our study on the continuous change of solvatochromic shifts of the chromophore acetone

* Corresponding author e-mail: gao@chem.umn.edu.

10.1021/ct700058c CCC: $37.00
Published on Web 06/14/2007

as a probe solute in fluid water by using a combined quantum mechanical configuration interaction and molecular mechanical potential in statistical mechanical Monte Carlo simulations.

Solvatochromic shifts of organic chromophores have been used extensively as a probe to investigate solute−solvent interactions in solution.[16−25] Based on the change in electronic absorption spectra of organic dye molecules, solvent polarity scales have been established including the popular $E_T(30)$ scale based on Reichardt's betaine dye.[16,26,27] One group of chromophores containing carbonyl, thiocarbonyl, and azo functional groups are often used, which have characteristically weak n → π* absorption bands.[16] Typically, a blue-shift in the absorption spectrum is observed in going from a low dielectric solvent to a more polar medium, although dispersion red-shifts are also found in nonpolar solvents such as carbon tetrachloride and hexane.[16,28−30]

Continuum solvation models coupled with electronic structure calculations have been widely used to model solvatochromic shifts.[18,20,31−34] The ZINDO program and its associated methods developed by Zerner have been applied to a variety of chromophores with remarkable success.[18] Cossi and Barone evaluated the n → π* transition of acetone in various polar and nonpolar solvents using the polarizable continuum solvation model,[31] while a number of other groups have also studied this system using different techniques.[20,33−40] Although excellent agreement with experiment can be obtained, a shortcoming of the continuum solvation approach is a lack of treating specific hydrogen bonding interactions. Zerner showed that only when one or two explicit water molecules are included, would the computed spectral shifts for a series of pyrimidine and pyrazine compounds be in accord with experiment.[18] On the other hand, combined QM/MM simulations even at the level of configuration interaction with single excitations (CIS) only can yield reasonable results.[22] Of course, the latter computations are much more time-consuming as it requires configurational averaging over millions of solvent configurations. Avoiding explicit electronic structure calculations, Warshel and co-workers used the partial charges derived for the ground and excited states along with an atom-centered polarizable dipole model to determine the solvent effects on vertical excitation energy.[41] This approach has been used by Blair et al.[42] and by DeBolt and Kollman et al.[43] in the analysis of excited-state energy relaxation. Previously, our group described a combined QM-CI/MM approach in Monte Carlo simulations, which has been applied to a number of systems, including acetone in a variety of solvents.[22−24,44,45] Later, the method was extended by incorporating a consistent treatment of the instantaneous electronic polarization between the solute and solvent in response to solute excitation.[23,46] Thompson and Schenter also presented a combined QM-CI/MM-pol model that includes polarization effects in the MM region and have applied it to study both ground and excited states.[47,48] In addition, Martin et al. presented a strategy using the mean-field approximation combining the QM/MM method to calculate the solvent shift of acetone in the ambient water.[40] A combined QM/MM strategy has also been implemented in CASSCF calculations.[25]

Bennett and Johnston carried out a most comprehensive experimental study and measured the entire range of solvatochromic shifts of the n → π* absorption band of acetone in vapor, fluid, and liquid water.[1] The experimental results showed that the spectral shifts can be divided into three regions. First, there is an initial phase of rapid increase in spectral shift, relative to the excitation energy of the isolated chromophore acetone in the gas phase, in the low-density steam region. This is followed by a plateau region near supercritical fluid conditions. Finally, as the fluid density increases toward the ambient value, the absorption energy increases quickly again. The existence of a plateau region near supercritical conditions has been proposed as a feature due to solvent clustering.[1,49,50] In a separate study, Takebayashi et al., who utilized NMR spectroscopy and Monte Carlo simulations, found similar features, which were attributed to the variations in solute−solvent hydrogen bonding as the temperature and water density changes.[51,52] On the theoretical side, a number of molecular dynamics and Monte Carlos simulations have been reported, primarily focusing on solute−solvent interactions at or near the supercriptical fluid region at a few selected states.[15,53−55] These studies provided support to solvent clustering at supercritical conditions. Recently a classical Monte Carlo simulation of acetone in water followed by cluster calculations with semiempirical and time-dependent density functional theory has been reported at the supercritical point,[37] and the change of solvatochromic shifts of an organic chromophore in the entire range of solvent densities has not been demonstrated computationally.

In this work, we aim to assess the solvent effects on the n → π* blue-shift of acetone in the full region from steam vapor to supercritical conditions to ambient water. The computed n → π* solvatochromic shifts of acetone in water fluids at various temperatures and solvent densities are compared with experimental values.[1] To evaluate the contributions of different molecular interactions to the acetone n → π* blue-shift in these fluid states, a decomposition analysis of the energies was computed based on the method our group developed previously.[23,46] To this end, statistical Monte Carlo simulations using a hybrid quantum-mechanical-configuration interaction and molecular mechanical (QM-CI/MM) method have been carried out to explore the solvent effects in electronic spectroscopy. The effects of the solvent polarization in response to the solute electronic excitation is evaluated by using a polarizable MM solvent model.[23,46,56] The results of the calculations reveal the factors governing the solvatochromic shifts of acetone at different water densities and temperatures, where a polarization correlation term from the instantaneous polarization of the solvent molecules following the solute excitation was also estimated. In the following, we first present the theoretical background and computational details. This is followed by results and discussion. Finally, the main findings are summarized in the conclusion.

Methods

We use a combined quantum mechanical-configuration interaction and molecular mechanical (QM-CI/MM) potential

in statistical mechanical Monte Carlo simulations to investigate the solvatochromic shifts in the n $\rightarrow \pi^*$ transition of acetone in fluid water.[22,23] In this hybrid system, the solute chromophore (i.e., acetone) is treated by a CI wave function, and the solvent molecules are represented classically by empirical potential functions.[22,47] Except for a few cases, most applications of combined QM/MM potentials make use of effective pairwise potentials for the MM region, in which the partial atomic charges on the solvent atoms are fixed at the same values both for the ground and excited states of the solute. This fixed-charge approach ignores the instantaneous charge polarization of the solvent due to solute electronic excitation, i.e., the interaction of the QM and solvent-induced dipoles, and the change in solvent configurations. In the present work, we also use a polarizable solvent model for water. Thus, the mutual "QM" solute and "MM" solvent polarization interactions are explicitly treated.[23,46−48] This is of particular interest in the present study because we examine the solvation of acetone by fluid water that covers the entire range of solvent densities, ranging from steam vapor to supercritical fluid to the dense liquid at the ambient condition. Previously we have implemented a polarizable combined QM/MM method for the study of electronic absorption in polar solvent,[23] and the approach is similar to another study described by Thompson and Schenter.[47,48] Here, we investigate solvation effects in supercritical fluids by including the instantaneous polarization of solvent molecules in response to the solute excited-state wave function.

Energy Decomposition. The total ground-state energy of the QM/MM hybrid system with the utilization of a polarizable solvent model can be written as follows[23,46,48]

$$E_{\mathrm{tot}}^{\mathrm{g}} = \langle \Phi_{\mathrm{CI}}^{\mathrm{g}} | \hat{\mathrm{H}}_{\mathrm{X}}^{\mathrm{o}} + \hat{\mathrm{H}}_{\mathrm{Xs}}^{\mathrm{stat}}(\{q_s\}) + \hat{\mathrm{H}}_{\mathrm{Xs}}^{\mathrm{pol}}(\{\mu_s^{\mathrm{g}}\}) | \Phi_{\mathrm{CI}}^{\mathrm{g}} \rangle + E_{\mathrm{Xs}}^{\mathrm{vdW}} + E_{ss}^{\mathrm{pair}} - \frac{1}{2}\sum_s \mu_s^{\mathrm{g}} \cdot \mathrm{F}_s^{\mathrm{o}} + \frac{1}{2}\sum_s \mu_s^{\mathrm{g}} \cdot \mathrm{F}_s^{\mathrm{qm}}(\{\Phi_{\mathrm{CI}}^{\mathrm{g}}\}) \quad (1)$$

where the superscript "g" signifies quantities for the solute in the ground state, $\Phi_{\mathrm{CI}}^{\mathrm{g}}$ is the ground state CI wave function of the solute, $\hat{H}_{\mathrm{X}}^{\mathrm{o}}$ is the Hamiltonian of the isolated solute (X), $\hat{H}_{\mathrm{Xs}}^{\mathrm{stat}}(\{q_s\})$ is the electrostatic interaction Hamiltonian between the QM system and the MM permanent charges (q_s), and$\hat{H}_{\mathrm{Xs}}^{\mathrm{pol}}(\{\mu_s^g\})$ is the interaction between the QM solute and the MM induced dipoles (μ_s^g) in the solute ground state. The remaining terms do not involve the electronic degrees of freedom, except the last term due to the fact that energy terms are not additive in a polarizable force field.[46] In eq 1, $E_{\mathrm{Xs}}^{\mathrm{vdW}}$ is the van der Waals interaction between the solute and solvent atoms, E_{ss}^{pair} is the solvent pair interaction consisting of both Lennard-Jones and Coulomb terms, F_s^{o} is the static electrostatic field from the MM system from its permanent charges, and $\mathrm{F}_s^{\mathrm{qm}}(\{\Phi_{\mathrm{CI}}^{\mathrm{g}}\})$ is the electrostatic field generated by the solute wave function. The induced dipoles of MM atoms s (μ_s^{g}) in eq 1 are determined self-consistently by an iterative procedure using eq 2[46,48]

$$\mu_s^{\mathrm{g}} = \alpha_s\left[\mathrm{F}_s^{\mathrm{o}} + \mathrm{F}_s^{\mathrm{qm}}(\{\Phi_{\mathrm{CI}}^{\mathrm{g}}\}) + \sum_{t\neq s} \nabla_s \nabla_t \left(\frac{1}{r_{st}}\right) \cdot \mu_t^{\mathrm{g}}\right] \quad (2)$$

where the subscripts (s,t) refer to MM atoms, α_s is the atomic polarizability of atom s, r_{st} is the distance between atoms s and t, and μ_t^{g} ($t \neq s$) are induced dipoles of all the other solvent. The value of $\{\mu_s^{\mathrm{g}}\}$ is a function of the permanent charges of the MM atom s, all other solvent-induced dipoles (μ_t^{g}, $t \neq s$) in the MM region, and the instantaneous external field from the QM system, $F_s^{\mathrm{qm}}(\{\Phi_{\mathrm{CI}}^{\mathrm{g}}\})$, which is derived from the molecular wave function of the solute. Since $\Phi_{\mathrm{CI}}^{\mathrm{g}}$ and $\{\mu_s^{\mathrm{g}}\}$ are dependent on each other, they must be solved self-consistently. We have employed a triple-iterative procedure to achieve the convergences of both the solute wave function and the solvent induced dipole, and of the overall mutually polarized system,[46,48] and the computational details have been described in refs 46 and 48. In short, we first use a set of induced solvent dipoles, which are kept frozen, along with the solvent permanent point charges to optimize the solute wave function. Then, the electric field of the solute molecule is included in eq 2 to optimize the solvent induced dipoles $\{\mu_s^{\mathrm{g}}\}$. The new set of $\{\mu_s^{\mathrm{g}}\}$ is again used to obtain an updated $\Phi_{\mathrm{CI}}^{\mathrm{g}}$. This process continues until the total energy of the entire system in eq 1 is fully converged.

For the excited state of the solute, a similar energy expression can be obtained[46,48]

$$E_{\mathrm{tot}}^{\mathrm{e}} = \langle \Phi_{\mathrm{CI}}^{\mathrm{e}} | \hat{\mathrm{H}}_{\mathrm{X}}^{\mathrm{o}} + \hat{\mathrm{H}}_{\mathrm{Xs}}^{\mathrm{stat}}(\{q_s\}) + \hat{\mathrm{H}}_{\mathrm{Xs}}^{\mathrm{pol}}(\{\mu_s^{\mathrm{e}}\}) | \Phi_{\mathrm{CI}}^{\mathrm{e}} \rangle + E_{\mathrm{Xs}}^{\mathrm{vdW}} + E_{ss}^{\mathrm{pair}} - \frac{1}{2}\sum_s \mu_s^{\mathrm{e}} \cdot \mathrm{F}_s^{\mathrm{o}} + \frac{1}{2}\sum_s \mu_s^{\mathrm{e}} \cdot \mathrm{F}_s^{\mathrm{qm}}(\{\Phi_{\mathrm{CI}}^{\mathrm{e}}\}) \quad (3)$$

where the superscript "e" indicates excited-state quantities, $\Phi_{\mathrm{CI}}^{\mathrm{e}}$ is the excited state CI wave function of the molecules in the QM region, and μ_s^{e} is the induced dipole of the solvent atom s in the MM region optimized in response to the presence of the QM solute in its electronically excited state. In eq 3, the solvent polarization is assumed to be instantaneous in response to the solute electronic excitation. In general, a similar triple-iterative procedure as that for the ground state can be used, but this is very time-consuming to optimize the excited-state wave function. Fortunately, it is typically not necessary. In the present work, a simplified procedure is adopted to solve the coupled QM- and MM-SCF calculations in eq 3:[46,48] we use the excited-state electric field of the solute, determined by the optimized ground-state reference wave function, to determine the solvent dipoles $\{\mu_s^{\mathrm{e}}\}$. Thus, we do not further optimize $\Phi_{\mathrm{CI}}^{\mathrm{e}}$. This is based on the Franck−Condon principle that the solvent and solute nuclei remain fixed in the Franck−Condon transition and the solvent's configuration can be approximated by that in the ground state.[28] The small perturbation of $\{\mu_s^{\mathrm{e}}\}$ by optimized $\Phi_{\mathrm{CI}}^{\mathrm{e}}$ is ignored because this is of third-order effects. Consequently, the QM/MM polarization term in eq 3 could be approximately defined as follows

$$\langle \Phi_{\mathrm{CI}}^{\mathrm{e}} | \hat{\mathrm{H}}_{\mathrm{Xs}}^{\mathrm{pol}}(\{\mu_s^{\mathrm{e}}\}) | \Phi_{\mathrm{CI}}^{\mathrm{e}} \rangle \approx \langle \Phi_{\mathrm{CI}}^{\mathrm{e}} | \hat{\mathrm{H}}_{\mathrm{Xs}}^{\mathrm{pol}}(\{\mu_s^{\mathrm{g}}\}) | \Phi_{\mathrm{CI}}^{\mathrm{e}} \rangle + \langle \Phi_{\mathrm{CI}}^{\mathrm{e}} | \hat{\mathrm{H}}_{\mathrm{Xs}}^{\mathrm{pol}}(\{\Delta\nu_s\}) | \Phi_{\mathrm{CI}}^{\mathrm{e}} \rangle \quad (4)$$

where $\Delta\nu_s = \mu_s^{\mathrm{e}} - \mu_s^{\mathrm{g}}$. In eq 4, the last term can be expressed classically for the interaction between the solvent-induced dipole with the QM electric field.

$$\langle \Phi_{CI}^{e} | \hat{H}_{Xs}^{pol}(\{\Delta\nu_s\}) | \Phi_{CI}^{e} \rangle = -\sum_s \Delta\nu_s \cdot F_s^{qm}(\{\Phi_{CI}^{e}\}) \quad (5)$$

We employ eqs 4 and 5 to rewrite eq 3 as

$$E_{tot}^{e} = \langle \Phi_{CI}^{e} | \hat{H}_X^o + \hat{H}_{Xs}^{stat}(\{q_s\}) + \hat{H}_{Xs}^{pol}(\{\mu_s^g\}) | \Phi_{CI}^{e} \rangle + E_{Xs}^{vdW} + E_{ss}^{pair} - \frac{1}{2}\sum_s \mu_s^e \cdot F_s^o + \frac{1}{2}\sum_s \mu_s^e \cdot F_s^{qm}(\{\Phi_{CI}^{e}\}) - \sum_s \Delta\nu_s \cdot F_s^{qm}(\{\Phi_{CI}^{e}\}) \quad (6)$$

The difference between eqs 3 and 6 is that the former involves fully iterative QM-CI and solvent-polarization SCF calculations, whereas the latter only requires the MM-SCF iteration to obtain μ_s^e. In eq 6, excited-state energies in the CI calculations are determined by using the ground-state, solvent-induced dipoles.[46,48] Therefore, the transition energy of the solute from the ground state to the excited state in solution can be obtained by subtracting eq 1 from eq 6

$$\Delta E_{tot}^{g\to e} = \langle \Phi_{CI}^{e} | \hat{H}_X^o + \hat{H}_{Xs}^{stat}(\{q_s\}) + \hat{H}_{Xs}^{pol}(\{\mu_s^g\}) | \Phi_{CI}^{e} \rangle - \langle \Phi_{CI}^{g} | \hat{H}_X^o + \hat{H}_{Xs}^{stat}(\{q_s\}) + \hat{H}_{Xs}^{pol}(\{\mu_s^g\}) | \Phi_{CI}^{g} \rangle - \frac{1}{2}\sum_s \Delta\nu_s \cdot F_s^o + \frac{1}{2}\sum_s [\mu_s^e \cdot F_s^{qm}(\{\Phi_{CI}^{e}\}) - \mu_s^g \cdot F_s^{qm}(\{\Phi_{CI}^{g}\})] - \sum_s \Delta\nu_s \cdot F_s^{qm}(\{\Phi_{CI}^{e}\}) \quad (7)$$

A further approximation of eq 7 is that we assume that the van der Waals terms for the solute in the ground state and the excited state are the same. Implicitly, we ignore the dispersion effects between solute and solvent in absorption spectral calculations.[29,30]

Explicit Simulation Studies. The excitation energy of a chromophore in solution as defined by eq 7 can be partitioned into two components as follows[46,57]

$$\Delta E_{tot}^{g\to e} = \Delta E_{stat}^{g\to e} + \Delta E_{pol}^{g\to e} \quad (8)$$

where

$$\Delta E_{stat}^{g\to e} = \langle \Phi_{CI}^{e} | \hat{H}_X^o + \hat{H}_{Xs}^{stat}(\{q_s\}) + \hat{H}_{Xs}^{pol}(\{\mu_s^g\}) | \Phi_{CI}^{e} \rangle - \langle \Phi_{CI}^{g} | \hat{H}_X^o + \hat{H}_{Xs}^{stat}(\{q_s\}) + \hat{H}_{Xs}^{pol}(\{\mu_s^g\}) | \Phi_{CI}^{g} \rangle \quad (9)$$

and

$$\Delta E_{pol}^{g\to e} = -\frac{1}{2}\sum_s \Delta\nu_s \cdot F_s^o + \frac{1}{2}\sum_s [\mu_s^e \cdot F_s^{qm}(\{\Phi_{CI}^{e}\}) - \mu_s^g \cdot F_s^{qm}(\{\Phi_{CI}^{g}\})] - \sum_s \Delta\nu_s \cdot F_s^{qm}(\{\Phi_{CI}^{e}\}) \quad (10)$$

In eq 9, $\Delta E_{stat}^{g\to e}$ represents the vertical excitation energy of the solute in the presence of the total electric field of the solvent that is equilibrated to the ground-state charge distribution of the solute. The remaining contributing terms in eq 10, $\Delta E_{pol}^{g\to e}$, indicate the correlation effects resulting from the instantaneous polarization of the solvent molecules by the solute excitation. The solvatochromic shift, $\Delta\nu$, is defined as the difference between the excitation energies of the chromophore in solution and in the gas phase

$$\Delta\nu = \langle \Delta E_{tot}^{g\to e} \rangle - \Delta E_{gas}^{g\to e} \quad (11)$$

where the bracket indicates an ensemble average over the Monte Carlo or molecular dynamics simulations. Making use of the energy partition in eq 7, we can formally separate the overall solvatochromic shift into two terms: (1) the spectral shift due to the solvent potential equilibrated to the ground state of the solute, $\langle \Delta\Delta E_{stat}^{g\to e} \rangle$ and (2) the subsequent energy change of the solvent dipole due to the solute electronic excitation. Thus,

$$\Delta\nu = \langle \Delta\Delta E_{stat}^{g\to e} \rangle + \Delta E_{pol}^{g\to e} \quad (12)$$

where

$$\langle \Delta\Delta E_{stat}^{g\to e} \rangle = \langle \Delta E_{stat}^{g\to e} \rangle - \Delta E_{gas}^{g\to e} \quad (13)$$

As described in our previous works,[23,46] the $\langle \Delta\Delta E_{stat}^{g\to e} \rangle$ term can be further decomposed into two components

$$\langle \Delta\Delta E_{stat}^{g\to e} \rangle = \langle \Delta E_{Xs}^{g\to e} \rangle + \langle \Delta\Delta E_{X}^{g\to e} \rangle \quad (14)$$

where $\Delta E_{Xs}^{g\to e}$ describes the energy change of the solute−solvent interaction due to the solute electronic excitation, and $\Delta\Delta E_X^{g\to e}$ depicts the difference between the excitation energy of the solute in the gas phase ($\Delta E_{X,gas}^{g\to e}$) and that in solution ($\Delta E_X^{g\to e}$):

$$\langle \Delta\Delta E_X^{g\to e} \rangle = \langle \Delta E_X^{g\to e} \rangle - \Delta E_{X,gas}^{g\to e} \quad (15)$$

The energy decomposition scheme of eqs 7 and 12 provides us with a convenient, approximate procedure for estimating the instantaneously mutual polarization effects upon solute electronic excitation. First, we carry out Monte Carlo or molecular dynamics simulations using an effective, pairwise potential for the solvent such as the four-point charge TIP4P models. Since polarization effects for the ground-state configurations have been included in the potential in an average sense, on average, the computed excitation energy using such a nonpolarizable model corresponds to the energy difference of eq 7, which is written for a polarizable solvent model, averaged over the Monte Carlo trajectories. Then, we switch the solvent potential to a polarizable model and use the configurations generated in the first step that employs a nonpolarizable, effective potential to determine the ensemble average of the effects (or energy contribution) of instantaneous polarization of the solvent in response to the solute excitation. This average yields the energy terms in eq 10.

Computational Details

All QM/MM calculations in statistical mechanical Monte Carlo simulations were performed using the MCQUB/MCQUM programs,[58,59] in which the quantum mechanical energies were calculated using the MOPAC program.[60] Monte Carlo simulations were carried out for a cubic box containing 396 water molecules and one acetone molecule with periodic boundary conditions. The isothermal isobaric (NPT) ensemble was employed at temperatures of 25, 50, 100, 200, 300, 400, 450, and 500 °C and pressures in the range of 1−2763 atm. These results in bulk conditions of a

reduced density (ρ_r) range from 0.05 to 3.10. A total of 29 unique conditions were included with various temperature and pressure conditions. The size has been shown to sufficiently describe thermodynamic and spectroscopic properties of solutes in SCW and the ambient water, especially at high-temperature regions where the fluid density is low.[13,15,51−55] The intermolecular interaction among water molecules was spherically truncated at 9 Å. The spherical cutoff distances of the solvent−solute interaction employed in these calculations were about one-half of the edge of each unit box, ranging from 10.07 to 41.94 Å. This is reasonable since the solute molecule is not charged or having significant charge separations. Nevertheless, it might be advisable to include long-range electrostatic effects in these simulations since the ability of solvent dielectric screening effects may be different in such a large density range. In all QM-CI/MM calculations, the acetone structure was held rigid at the AM1 geometry optimized in the gas phase.[61] The electronic excited-state calculations were performed by configuration interaction that includes a total of 100 configurations from an active space of 6 electrons in 5 orbitals, and these combinations have been shown to yield excellent results for acetone even though the model was not originally developed for spectroscopy.[22,30] The van der Waals parameters for the QM atoms were determined in a previous study.[62]

Two separate calculations were executed. First, the combined QM-CI/MM potential with the pairwise four-point charge TIP4P water model[63] was utilized to yield the average values for $\langle \Delta E_{stat}^{g\rightarrow e} \rangle$. The TIP4P model has been verified to adequately describe the properties of SCW for the present purposes.[15,54] In particular, a series of Monte Carlo simulations has been carried out at 400 °C and pressures ranging from 350 to 2000 atm. By analysis of reduced parameters, it was suggested that the TIP4P model may slightly underestimate the supercritical temperature by 30 to 50 degrees.[15] In the second set of QM-CI/MM simulations, the polarizable POL2 model[56] was adopted for the MM solvent to give the polarization correlation energy, $\Delta E_{pol}^{g\rightarrow e}$. In this step, only the single-point energies were evaluated based on the configurations generated in the first set of simulation. Each Monte Carlo simulation in the first computational step involves at least 4×10^6 configurations of equilibration, followed by 4×10^6 configurations for data averaging. The Owicki-Scheraga preferential sampling technique was used to enhance the statistics near the solute, such that solvent moves are made proportional to $1/(R^2 + W)$, where $W =$ 350 Å.[64] The averages for $\Delta E_{pol}^{g\rightarrow e}$ in the latter calculations were equilibrated for at least 4×10^6 configurations, followed by single-point energy evaluations with a total of 50 structures to obtain the instantaneous polarization response by the solvent. Note that all spectral shifts correspond to Franck−Condon excitation, in which solute and solvent electronic polarization are assumed to be instantaneous in the excited state at the solvent nucleus positions equilibrated to the ground-state electronic structures.

Results and Discussion

Solvatochromic Shifts. The total solvatochromic shift ($\Delta\nu$) for n → π^* excitation of acetone in water fluid calculated by the QM-CI/MM method is plotted as a function of reduced density (ρ_r) of the fluid in the range from 0.02 to 3.11 (Figure 1). The reduced density of 3.11 corresponds to simulations at 25 °C and 1 atm. The theoretical results show that the initial increase in the reduced density (ρ_r) from 0.02 to 0.7 is accompanied by a rapidly rising blue-shift in $\Delta\nu$. This is followed by a slowly rising plateau region in the reduced density range of 0.7−1.5. In the third stage, the increase of $\Delta\nu$ becomes markedly steeper at higher reduced densities from 1.5 to 3.1. The trend of $\Delta\nu$ obtained in the calculations is in excellent agreement with the experimental data reported by Bennett and Johnston.[1] The three distinctive regions in Figure 1 can be categorized as (1) the *gaseous steam phase* corresponding to a temperature of 500 K and pressures of 49 → 454 atm used in the Monte Carlo simulation, (2) the *supercritical fluid region* ($T = 400-500$ K and $P = 454-987$ atm), and (3) the *dense-liquid phase* ($T = 25-400$ K and $P = 1-2763$ atm). The plateau in the UV-absorption energy in the SCW region has been attributed to the effect of solvent clustering near the solute, which plays an important role in determining the chemical reactivity of organic solute in SCW.[65−67] The experimental observation is nicely reproduced here,[1] and we shall present structural analysis in the following section.

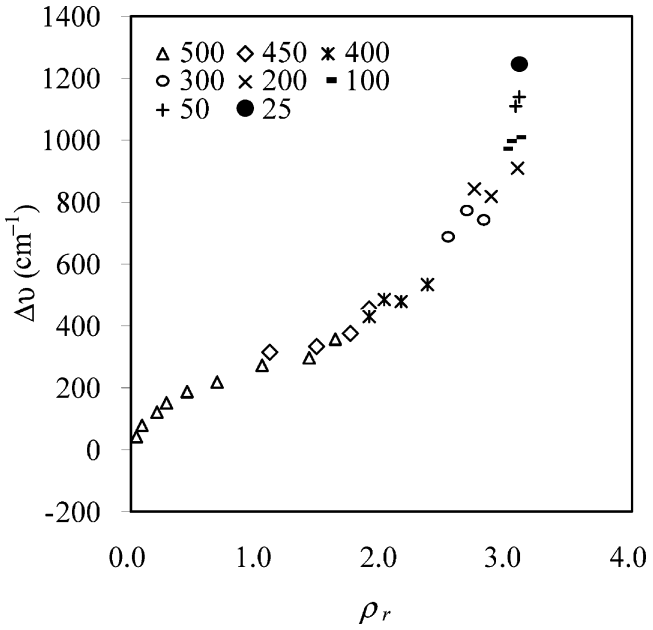

Figure 1. Computed solvatochromic shift ($\Delta\upsilon$) in the n → π^* excitation of acetone in water fluid as a function of reduced density (ρ_r). Temperatures in degrees Celsius used for different simulations are given in the upper left-hand corner.

The quality of the present study is best illustrated by the computed n → π^* spectral shift ($\Delta\nu$) for acetone in ambient water, which is 1245 cm^{-1}. For comparison, the experimental value is 1560 cm^{-1},[28,68] and the difference corresponds to an energy difference of only 0.9 kcal/mol. In an early study, the computed spectral shift is somewhat greater at 1690 cm^{-1};[22] the slight difference between with the present simulations may be a reflection of the difference in size and length of different simulations, but the trends within each individual set of calculations should be reseasonble. Solvatochromic shifts of acetone in various solvents have been

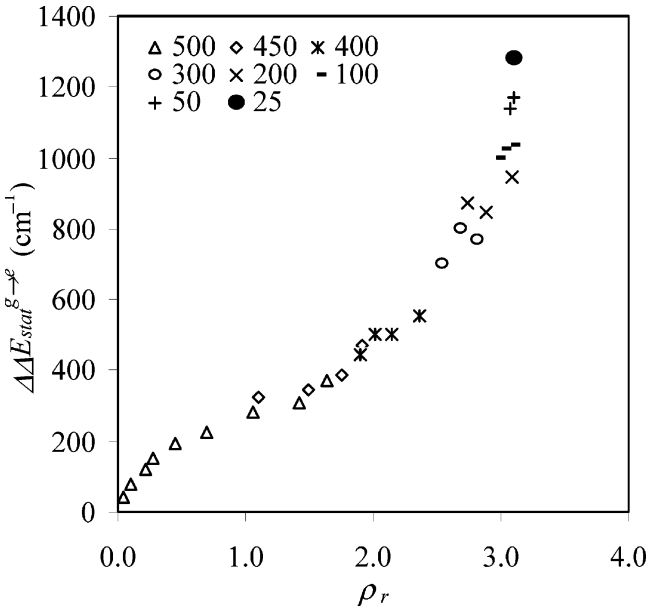

Figure 2. Electrostatic stabilization energy ($\Delta\Delta E_{stat}^{g\to e}$) due to ground-state solvent charge distribution for the n → π* excitation of acetone in water fluid as a function of fluid reduced density (ρ_r). Temperatures in degrees Celsius used for different simulations are given in the upper left-hand corner.

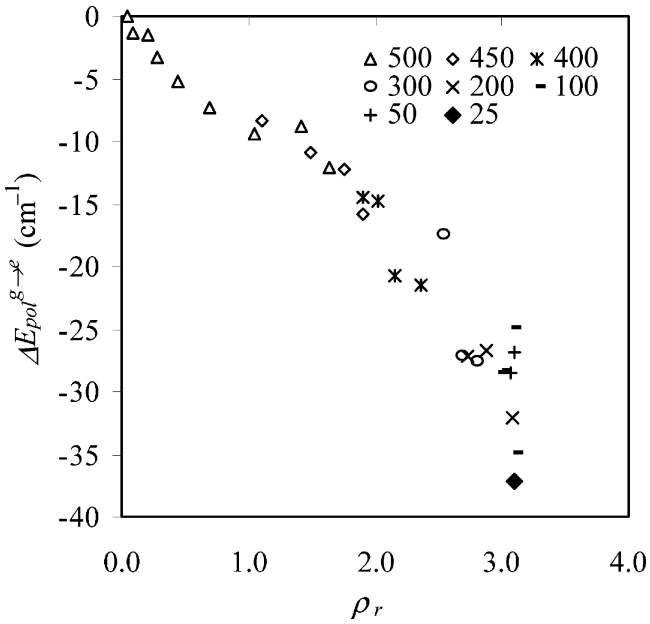

Figure 3. Computed solvent polarization contributions ($\Delta E_{pol}^{g\to e}$) to the overall spectral shifts for the n → π* excitation of acetone in water fluid as a function of fluid reduced density (ρ_r). Temperatures in degrees Celsius used for different simulations are given.

extensively investigated in ambient conditions.[22,30,32,39,48,69−72] It provides a prototypical system for studying solvation effects. The excellent agreement between the theoretical results and the experimental data indicates that the Monte Carlo simulations combined with the AM1 Hamiltonian for the QM atoms employed in the present work are adequate for analyses of the solvation structure and solvation energies of an organic solute in water fluids spanning the entire density ranges from vapor to supercritical fluids to dense liquid.

Energy Decompositions. To gain insight into the origin of the observed absorption spectral shifts and the possibility of solvent clustering near supercritical fluid conditions, we decomposed the total solvatochromic shifts into specific terms. If there is stable solvent cluster formation near the supercritical point, one would expect to find a relatively large and invariant condition from the $\Delta E_{pol}^{g\to e}$ term because the solvent polarization effects depend on the size of the cluster. To conveniently analyze the solvatochromic shift ($\Delta\nu$ of the acetone excitation in water fluid, the water reduced density (ρ_r) in this work is divided into four regions: the vapor phase ($\rho_r < 0.7$), the supercritical and near supercritical fluid region ($0.7 < \rho_r < 1.9$), the dense-liquid region ($\rho_r > 1.9$), and the ambient water state ($\rho_r = 3.11$).[1] In these four regions, the values of $\Delta\nu$ obtained from the hybrid QM-CI/MM calculations are in the range of 48−219 cm^{-1}, 273−452 cm^{-1}, 485−1142 cm^{-1}, and 1245 cm^{-1}, respectively (Figure 1).

$\Delta\nu$ can be decomposed into $\Delta\Delta E_{stat}^{g\to e}$ and $\Delta E_{pol}^{g\to e}$ terms (eq 11). The first term represents the electrostatic stabilization of the ground state over the excited state due to solvation, of which the excitation energy in solution is obtained using the solvent charge distribution in the ground state of the solute. The second term is the polarization correlation energy due to the instantaneous solvent polarization following the

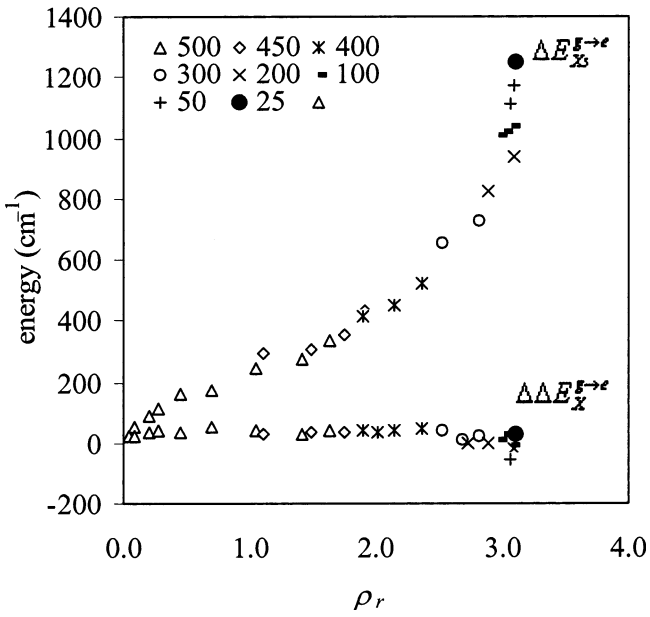

Figure 4. Decomposition of the ground-state electrostatic energy term in Figure 2 into the change in net solute−solvent interaction energy ($\Delta E_{Xs}^{g\to e}$) and the intrinsic excitation energy of the solute ($\Delta\Delta E_X^{g\to e}$) for the n → π* transition of acetone in water fluid. Temperatures in degrees Celsius used for different simulations are indicated.

solute electronic excitation. The decomposition results of $\Delta\nu$ show that in the vapor, supercritical and near supercritical fluid, dense-liquid, and the ambient water regions, $\Delta\Delta E_{stat}^{g\to e}$ contributes to the blue-shifts $\Delta\nu$ by 40−226 cm^{-1}, 282−468 cm^{-1}, 500−1169 cm^{-1}, and 1282 cm^{-1}, respectively (Figure 2). On the other hand, $\Delta E_{pol}^{g\to e}$ contributes a small red-shift to $\Delta\nu$ in ranges of −0.02 to −7 cm^{-1}, −8 to −16 cm^{-1}, −15 to −35 cm^{-1}, and −37 cm^{-1}, respectively (Figure

Table 1. Theoretical Results of Ground-State Dipole Moment in Water Fluid ($\langle\mu^g\rangle$),[a] Ground-State Induced Dipole Moment ($\Delta\mu^g_{ind}$),[b] Excited-State Dipole Moment in Water Fluid ($\langle\mu^e\rangle$), and Excited-State Induced Dipole Moment ($\Delta\mu^e_{ind}$)[c] for Acetone in the Supercritical ($\rho_r < 0.7$), Near-Critical ($0.7 < \rho_r < 1.9$) and Dense-Liquid Regions ($\rho_r > 1.9$) and Ambient Water ($\rho_r = 3.1$)

	$\langle\mu^g\rangle$ (D)	$\Delta\mu^g_{ind}$ (D)	$\langle\mu^e\rangle$ (D)	$\Delta\mu^e_{ind}$ (D)
supercritical region	2.94−3.17	0.02−0.25	2.89−3.06	0.02−0.19
near-critical region	3.21−3.41	0.29−0.49	3.15−3.36	0.28−0.49
dense-liquid region	3.42−3.98	0.51−1.06	3.34−3.95	0.47−1.08
ambient water	4.07	1.15	3.87	1.00

[a] Ensemble average of AM1 ground-state dipole moment in water fluid. [b] $\Delta\mu^g_{ind} = \langle\mu^g\rangle - \mu^g_{gas}$, where μ^g_{gas}, a value of 2.91 D, is the ground-state dipole moment of acetone using the optimized AM1 geometry in the gas phase. [c] $\Delta\mu^e_{ind} = \langle\mu^e\rangle - \mu^e_{gas}$, where μ^e_{gas}, a value of 2.87 D, is the excited-state dipole moment of acetone in the gas phase.

3). Clearly, inclusion of the solvent instantaneous polarization effects leads to stabilization of the electronic excited state, giving rise to a red-shift in the absorption energy, and the effect increases as the solvent density increases. However, it only makes a small correction to the total solvatochromic shift, suggesting that that the energy input required to reorient solvent dipoles following the solute excitation is small.

To further understand the solute−solvent interactions and the solute intrinsic energy contributing to the electrostatic stabilization over the excitation due to solvation ($\Delta\Delta E^{g\to e}_{stat}$), the $\Delta\Delta E^{g\to e}_{stat}$ term is further separated into $\Delta E^{g\to e}_{Xs}$ and $\Delta\Delta E^{g\to e}_{X}$, two terms using eq 14. The $\Delta E^{g\to e}_{Xs}$ represents the energy change of the solute−solvent interaction due to different solute charge distributions in the ground state and excited state, and $\Delta\Delta E^{g\to e}_{X}$ is the change of the intrinsic excitation energy of the solute in solution. In the vapor, supercritical and near supercritical, dense-liquid and ambient states, the energy component of $\Delta E^{g\to e}_{Xs}$ is the dominant component of the total solvatochromic shift, and the computed values are 23−167 cm^{-1}, 256−394 cm^{-1}, 484−1110 cm^{-1}, and 1253 cm^{-1}, respectively (Figure 4). Together with the solvent polarization correction, $\Delta E^{g\to e}_{pol}$, we find that the observed spectral shifts nearly come entirely from the difference in solute−solvent interaction energy between the excited and the ground states, comprising 95% of the total $\Delta\nu$. Surprisingly, the intrinsic excitation energy of the solute does not change significantly relative to the gas-phase value, with the computed $\Delta\Delta E^{g\to e}_{X}$ less than 50 cm^{-1} in all density ranges (Figure 4). Evidently, the polarization of the solute wave fuction does not affect the energy gap between the ground state and the $n \to \pi^*$ excited state. The results of the energy decompositions for the solvatochromic shift of the acetone $n \to \pi^*$ excitation reveal that the electrostatic stabilization from the solute−solvent interaction in the ground state over that in the excited state ($\Delta E^{g\to e}_{Xs}$) primarily dominates the spectra blue-shift. Furthermore, $\Delta E^{g\to e}_{Xs}$ increases continuously without a plateau behavior in SCW region, although it shows a clear transition in that region, leading to a rapid increase as the solvent density further increases (Figure 4). It is interesting to comment that for systems involving $\pi \to \pi^*$ transitions where dispersion and inductive polarization effects might be more significant, the quantitative picture could have greater polarization and intrinsic energy contributions. It would be interesting to make similar analyses of these types of compounds.

Dipole Moment vs Spectra Shift. A further measure of the molecular polarization is provided by calculating the ground-state and excited-state induced dipole moments of acetone due to solvation (Table 1). The calculated average and induced dipole moments continuously increase as the fluid density increases, whereas the values of $\langle\mu^g\rangle$ - $\langle\mu^e\rangle$ are relatively small. Thus, although the ground state is more strongly solvated than the excited state, the similarity in the computed dipoles in Table 1 show that specific solute−solvent interactions are critically important in molecular solvation, and the overall dipole moment of a molecule is not a direct indication of its strength of solvation.

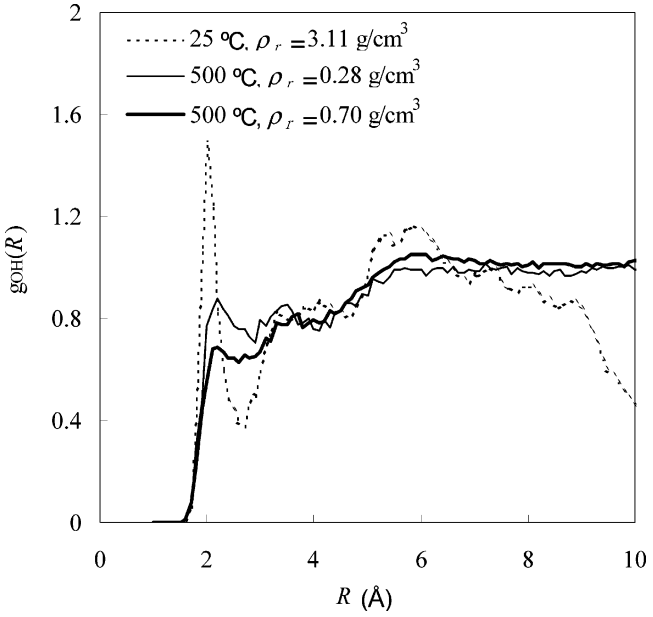

Figure 5. Computed radial-distribution functions for the acetone oxygen and water hydrogen ($g_{OH}(R)$) in ambient water (dashed line) and in the supercritical water states of 500 °C (solid lines).

Table 2. Computed Positions of the First Peaks (r_1) in Radial Distribution Functions (rdfs) and Coordination Numbers of Water Molecules in the First Solvation Shell of Acetone (N_{H_2O}) in the Supercritical, Near-Critical, Dense-Liquid, and Ambient Water Fluids

	r_1 (Å)	N_{H_2O}
supercritical region	2.1−2.3	0.08−0.72
near-critical region	2.1−2.3	0.61−1.44
dense-liquid region	2.0−2.2	1.22−2.51
ambient water	2.0	2.90

Solvent Structure vs Spectral Shift. The structural interpretation of energy component analyses is confirmed

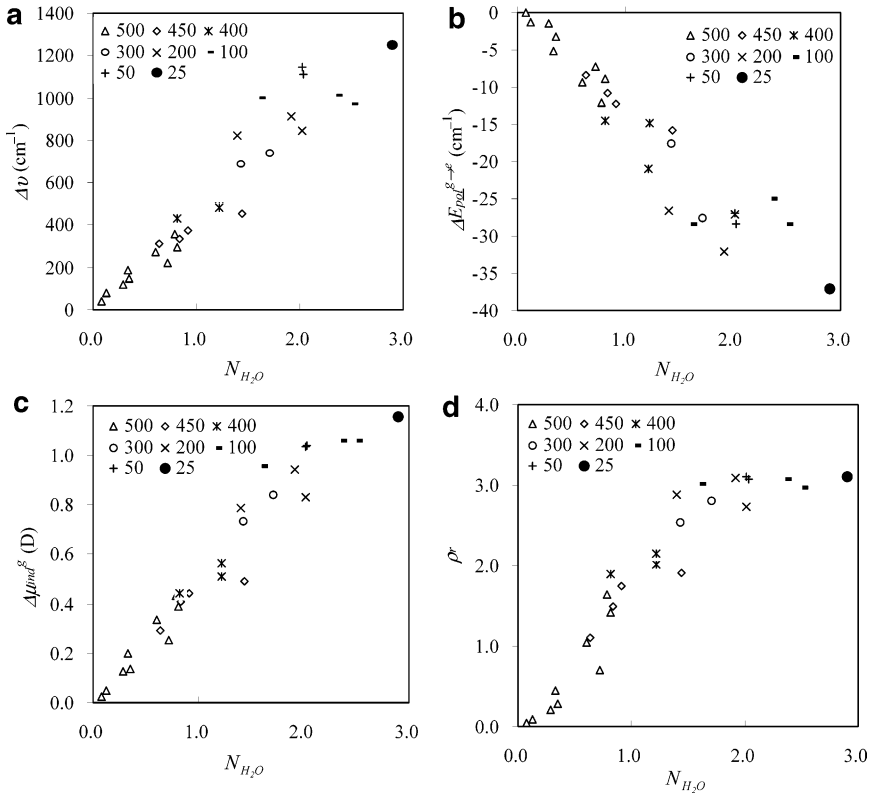

Figure 6. Correlations with the computed coordination number of water molecules in the first-solvation layer of acetone (N_{H_2O}) for (a) solvatochromic shift ($\Delta\nu$), (b) solvent polarization contribution ($\Delta E_{pol}^{g\rightarrow e}$), (c) ground-state induced dipole moment of acetone ($\Delta\mu_{ind}^{g}$), and (d) reduced density (ρ_r) of fluid. Temperatures in degrees Celsius used for different simulations are indicated.

by examining the radial distribution functions (rdfs) between the solute and solvent. In particular, we focus on the acetone oxygen (O) and the water hydrogen (Hw) rdf, $g_{OH}(R)$, which gives the probability of finding a water hydrogen atom (Hw) at a distance R from the acetone oxygen (O). Figure 5 shows the rdfs obtained in the ambient water (T = 25 °C, ρ_r = 3.11) and a state just above the supercritical conditions of 500 °C at a reduced density of 0.70. Table 2 presents the positions of the first peaks of the rdfs and the coordination number of water molecules in the first solvation layer for acetone in these four water conditions. In the ambient water, the position of the first solvation peak is well-defined appearing at 2.0 Å, but the second peak is less structured. The calculated solvent structure in the ambient water is similar to that observed by Thompson,[48] by Takebayashi et al.,[51,52] and by Martin et al.[40] In contrast, there is no well-defined first peak of $g_{OH}(R)$ in the supercritical conditions (Figure 5), which is also in accord with the results obtained by Takebayashi et al.[51,52]

The positions of the first peak of $g_{OH}(R)$ in the vapor, supercritical and near supercritical, and dense-liquid water fluids were shifted to longer distances in comparison with that in ambient water by 0.1−0.3 Å, 0.1−0.3 Å, and 0.0−0.2 Å, respectively (Table 2). Furthermore, the coordination numbers in the first solvation layer about the oxygen of acetone (N_{H_2O}) are 0.08−0.72, 0.61−1.44, and 1.22−2.51 in the corresponding conditions (Table 2 and Figure 6d). These results show that the average number of N_{H_2O} is an increasing function of water density, which is consistent with the finding by Takebayashi et al.[51,52] It is worthy to note that the trend of the coordination numbers of water (N_{H_2O}) in the first layer around acetone reflects the total solvatochromic shifts ($\Delta\nu$ in the n → π^* excitation of acetone with a linear correlation of r^2 = 0.91 (Figure 6a). The solvent polarization correction ($\Delta E_{pol}^{g\rightarrow e}$) and the ground-state induced dipole ($\Delta\mu_{ind}^{g}$) also show linear correlations with N_{H_2O} (Figure 6b,c). Overall, it implies that the density-dependent N_{H_2O} of specific hydrogen-bond interactions between acetone and water molecules directly influences the magnitude of the solvatochromic shift, solvent polarization correction, and the induced dipole of acetone. In fact, the changes in coordination number shown in Figure 6d as a function of the fluid reduced density mirrors completely with the trends of the spectral shifts in Figure 1.

Conclusions

Hybrid QM-CI/MM Monte Carlo simulations have been carried out to investigate the solvatochromic shifts of the acetone n → π^* excitation in the supercritical (ρ_r < 0.7), near-critical (0.7 < ρ_r < 1.9), dense-liquid (ρ_r > 1.9), and ambient water conditions. In the present work, the solvent polarization correlation following the solute electronic excitation was included. The computed n → π^* blue-shift in ambient water (1245 cm^{-1}) is in reasonable agreement with the experimental value ($\Delta\nu_{exp}$ = 1560 cm^{-1}).[28,68] The trend of the solvatochromic shift as a function of reduced fluid density with the range from 0.05 to 3.11 was in accord with the experiment probed by the UV−visible absorption spec-

troscopy.[1] The results of energy decomposition show that the solvatochromic shifts in the supercritical, near-critical, dense-liquid, and ambient water fluids are mainly determined by the electrostatic interactions between acetone and water molecules during the solute excitation. Furthermore, the energy required to orient solvent molecules following the acetone excitation is quite small and decreases linearly with water density. The solvent-density dependent blue-shift and the solvent polarization correction for the acetone $n \rightarrow \pi^*$ excitation in water fluid are governed by the induced dipole of acetone in the ground and excited states and the specific hydrogen-bond interactions between the oxygen of acetone and the hydrogen of water. In addition, both energy terms are more obvious in the ambient water than in the supercritical water because the solvent stabilization of the ground state over the excited state is more significant in the former condition.

Acknowledgment. This work has been supported in part by the National Institutes of Health (GM46736) and by the Army Research Laboratory through the Army High-Performance Computing Research Center (AHPCRC) under the auspices of Army Research Laboratory DAAD 19-01-2-0014 and by the Office of Naval Research under grant number N00014-05-1-0538.

References

(1) Bennett, G. E.; Johnston, K. P. *J. Phys. Chem.* **1994**, *98*, 441.

(2) Bermejo, M. D.; Cocero, M. J. *AIChE J.* **2006**, *52*, 3933.

(3) Marrone, P. A.; Hodes, M.; Smith, K. A.; Tester, J. W. *J. Supercrit. Fluids* **2004**, *29*, 289.

(4) Marrone, P. A.; Cantwell, S. D.; Dalton, D. W. *Ind. Eng. Chem. Res.* **2005**, *44*, 9030.

(5) Ryan, E. T.; Xiang, T.; Johnston, K. P.; Fox, M. A. *J. Phys. Chem. A* **1997**, *101*, 1827.

(6) Williams, P. T.; Onwudili, J. A. *Environ. Technol.* **2006**, *27*, 823.

(7) Shaw, R. W.; Brill, T. B.; Clifford, A. A.; Eckert, C. A.; Franck, E. U. *Chem. Eng. News* **1991**, *69* (51), 26.

(8) Savage, P. E. *Chem. Rev.* **1999**, *99*, 603.

(9) Minett, S.; Fenwick, K. *Eur. Water Manage.* **2001**, *4*, 54.

(10) Haar, L.; Gallagher, J. S.; Kell, G. S. *NBSATRC Steam Tables*; Hemisphere: Washington, DC, 1984.

(11) Archer, D. G.; Wang, P. *J. Phys. Chem. Reg. Data* **1990**, *19*, 371.

(12) Paulaitis, M. E.; Krukonis, V. J.; Kurnik, R. T.; Reid, R. C. *Rev. Chem. Eng.* **1983**, *1*, 179.

(13) Johnston, K. P.; Rossky, P. J. *NATO Sci. Ser. Ser. E* **2000**, *366*, 323.

(14) Galkin, A. A.; Lunin, V. V. *Russ. Chem. Rev.* **2005**, *74*, 21.

(15) Gao, J. *J. Am. Chem. Soc.* **1993**, *115*, 6893.

(16) Reichardt, C. *Solvents and Solvent Effects in Organic Chemistry*, 2nd ed.; VCH: Weinheim, 1990.

(17) Amos, A. T.; Hall, G. G. *Proc. R. Soc. London, Ser. A* **1961**, *263*, 482.

(18) (a) Karelson, M. M.; Katritzky, A. R.; Zerner, M. C. *Int. J. Quantum Chem., Quantum Chem. Symp.* **1986**, *20*, 521. (b) Karelson, M. M.; Zerner, M. C. *J. Am. Chem. Soc.* **1990**, *112*, 9405. (c) Karelson, M. M.; Zerner, M. C. *J. Phys. Chem.* **1992**, *96*, 6949.

(19) Lerf, C.; Suppan, P. *J. Chem. Soc. Faraday Trans.* **1992**, *88*, 963.

(20) Li, J.; Cramer, C. J.; Truhlar, D. G. *Int. J. Quantum Chem.* **2000**, *77*, 264.

(21) Nugent, S.; Ladanyi, B. M. *J. Chem. Phys.* **2004**, *120*, 874.

(22) Gao, J. *J. Am. Chem. Soc.* **1994**, *116*, 9324.

(23) Gao, J.; Byun, K. *Theor. Chem. Acc.* **1997**, *96*, 151.

(24) Rajamani, R.; Gao, J. *J. Comput. Chem.* **2002**, *23*, 96.

(25) Poulsen, T. D.; Ogilby, P. R.; Mikkelsen, K. V. *J. Chem. Phys.* **2002**, *116*, 3730.

(26) Buncel, E.; Rajagopal, S. *Acc. Chem. Res.* **1990**, *23*, 226.

(27) Reichardt, C. *Chem. Rev.* **1994**, *94*, 2319.

(28) Bayliss, N. S.; McRae, E. G. *J. Phys. Chem.* **1954**, *58*, 1006.

(29) Canuto, S.; Coutinho, K.; Zerner, M. C. *J. Chem. Phys.* **2000**, *112*, 7293.

(30) Roesch, N.; Zerner, M. C. *J. Phys. Chem.* **1994**, *98*, 5817.

(31) Cossi, M.; Barone, V. *J. Chem. Phys.* **2000**, *112*, 2427.

(32) Pappalardo, R. R.; Reguero, M.; Robb, M. A.; Frish, M. *Chem. Phys. Lett.* **1993**, *212*, 12.

(33) Minezawa, N.; Kato, S. *J. Chem. Phys.* **2007**, *126*, 054511/1.

(34) Mennucci, B.; Cammi, R.; Tomasi, J. *J. Chem. Phys.* **1998**, *109*, 2798.

(35) Martin, M. E.; Sanchez, M. L.; Olivares del Valle, F. J.; Aguilar, M. A. *J. Chem. Phys.* **2000**, *113*, 6308.

(36) Bernasconi, L.; Sprik, M.; Hutter, J. *J. Chem. Phys.* **2003**, *119*, 12417.

(37) Fonseca, T. L.; Coutinho, K.; Canuto, S. *J. Chem. Phys.* **2007**, *126*, 034508.

(38) Neugebauer, J.; Louwerse, M. J.; Baerends, E. J.; Wesolowski, T. A. *J. Chem. Phys.* **2005**, *122*, 094115.

(39) Coutinho, K.; Canuto, S. *THEOCEHEM* **2003**, *632*, 235.

(40) Martin, M. E.; Sanchez, M. L.; Olivares del Valle, F. J.; Aguilar, M. A. *J. Chem. Phys.* **2000**, *113*, 6308.

(41) Luzhkov, V.; Warshel, A. *J. Am. Chem. Soc.* **1991**, *113*, 4491.

(42) Blair, J. T.; Krogh-Jespersen, K.; Levy, R. M. *J. Am. Chem. Soc.* **1989**, *111*, 6948.

(43) DeBolt, S. E.; Kollman, P. A. *J. Am. Chem. Soc.* **1990**, *112*, 7515.

(44) Gao, J.; Li, N.; Freindorf, M. *J. Am. Chem. Soc.* **1996**, *118*, 4912.

(45) Gao, J.; Alhambra, C. *J. Am. Chem. Soc.* **1997**, *119*, 2962.

(46) Gao, J. *J. Comput. Chem.* **1997**, *18*, 1061.

(47) Thompson, M. A.; Schenter, G. K. *J. Phys. Chem.* **1995**, *99*, 6374.

(48) Thompson, M. A. *J. Phys. Chem.* **1996**, *100*, 14492.

(49) Heitz, M. P.; Bright, F. V. *J. Phys. Chem.* **1996**, *100*, 6889.

(50) Wyatt, V. T.; Bush, D.; Lu, J.; Hallett, J. P.; Liotta, C. L.; Eckert, C. A. *J. Supercrit. Fluids* **2005**, *36*, 16.

(51) Takebayashi, Y.; Sugeta, S. Y., T.; Otake, K.; Nakahara, M. *J. Phys. Chem. B* **2003**, *107*, 9847.

(52) Takebayashi, Y.; Yoda, S. S., T.; Otake, K.; Sako, T.; Nakahara, M. *J. Chem. Phys.* **2004**, *120*, 6100.

(53) Balbuena, P. B.; Johnston, K. P.; Rossky, P. J. *J. Phys. Chem.* **1996**, *100*, 2716.

(54) Gao, J. *J. Phys. Chem.* **1994**, *98*, 6049.

(55) Kubo, M.; Levy, R. M.; Rossky, P. J.; Matubayasi, N.; Nakahara, M. *J. Phys. Chem. B* **2002**, *106*, 3979.

(56) Dang, L. X. *J. Chem. Phys.* **1992**, *97*, 2659.

(57) Gao, J. *J. Phys. Chem.* **1992**, *96*, 537.

(58) Gao, J. *MCQUB; v3.0*; Department of Chemistry, SUNY: Buffalo, NY, 1998.

(59) Gao, J. *MCQUM; v4.0*; Department of Chemistry, University of Minnesota: Minneapolis, MN, 2000.

(60) Stewart, J. J. P. *J. Comput.-Aided Mol. Des.* **1990**, *4*, 1.

(61) Dewar, M. J. S.; Zoebisch, E. G.; Healy, E. F.; Stewart, J. J. P. *J. Am. Chem. Soc.* **1985**, *107*, 3902.

(62) Gao, J.; Xia, X. *Science* **1992**, *258*, 631.

(63) Jorgensen, W. L.; Chandrasekhar, J.; Madura, J. D.; Impey, R. W.; Klein, M. L. *J. Chem. Phys.* **1983**, *79*, 926.

(64) Owicki, J. C.; Scheraga, H. A. *Chem. Phys. Lett.* **1977**, *47*, 600.

(65) Westacott, R. E.; Johnston, K. P.; Rossky, P. J. *J. Am. Chem. Soc.* **2001**, *123*, 1006.

(66) Westacott, R. E.; Johnston, K. P.; Rossky, P. J. *J. Phys. Chem. B* **2001**, *105*, 6611.

(67) Balbuena, P. B.; Johnston, K. P.; Rossky, P. J.; Hyun, J.-K. *J. Phys. Chem. B* **1998**, *102*, 3806.

(68) Suppan, P. *J. Photochem. Photobiol.* **1990**, *A50*, 293.

(69) De Vries, A. H.; Van, Duijnen, P. T. *Int. J. Quantum Chem.* **1996**, *57*, 1067.

(70) Fox, T.; Roesch, N. *Chem. Phys. Lett.* **1992**, *191*, 33.

(71) Georg, H. C.; Coutinho, K.; Canuto, S. *Chem. Phys. Lett.* **2006**, *429*, 119.

(72) Roehrig, U. F.; Frank, I.; Hutter, J.; Laio, A.; VandeVondele, J.; Rothlisberger, U. *ChemPhysChem* **2003**, *4*, 1177.

CT700058C